

## Band Edge Model of (101)-Biaxial Strained Si\*

Song Jianjun<sup>†</sup>, Zhang Heming, Dai Xianying, Hu Huiyong, and Xuan Rongxi

(Key Laboratory of the Ministry of Education for Wide Band-Gap Semiconductor Materials and Devices, School of Microelectronics, Xidian University, Xi'an 710071, China)

**Abstract:** A band edge model in (101)-biaxial strained Si on relaxed Si<sub>1-x</sub>Ge<sub>x</sub> alloy, or monoclinic Si (m-Si), is presented using the  $k \cdot p$  perturbation method coupled with deformation potential theory. Results show that the [001], [00 $\bar{1}$ ], [100], [ $\bar{1}$ 00] valleys constitute the conduction band (CB) edge, which moves up in electron energy as the Ge fraction ( $x$ ) increases. Furthermore, the CB splitting energy is in direct proportion to  $x$  and all the valence band (VB) edges move up in electron energy as  $x$  increases. In addition, the decrease in the indirect bandgap and the increase in the VB edge splitting energy as  $x$  increases are found. The quantitative data from the models supply valuable references for the design of the devices.

**Key words:** strained Si; band edge;  $k \cdot p$  method

**PACC:** 7360F; 7125C; 7115M

**CLC number:** O471.5

**Document code:** A

**Article ID:** 0253-4177(2008)09-1670-04

### 1 Introduction

Engineering the band structure of semiconductor materials is an additional way to improve device performance. Such a material is the strained Si (s-Si) pseudomorphically grown on relaxed Si<sub>1-x</sub>Ge<sub>x</sub> (SiGe) substrate<sup>[1~3]</sup>. Si film that is subjected to varying degree of strain can be achieved using differently oriented substrates. Strain induced by the lattice mismatch between the Si layer and the SiGe substrate change the band structure and the electronic properties of Si significantly. Many applications of devices fabricated using s-Si constitute a considerable enhancement of the presently well-established Si technology. Due to the applications and the efficient design of devices fabricated using s-Si, it is necessary to study the band structure in s-Si, especially the band edge. S-Si grown on (101) oriented SiGe, or monoclinic Si (m-Si), is of particular interest since no reported results for it were found.

The band edge of m-Si can be obtained using various approaches: the pseudopotential method, the linear combination of atomic orbitals (LCAO) approach, the free-electron approximation method, and the  $k \cdot p$  perturbation method (sometimes referred to as the effective-mass method). The most powerful approach is the  $k \cdot p$  perturbation method coupled with deformation potential theory because it provides sufficiently high accuracy and is fairly easy to apply. Hence, we calculate the band edge level in m-Si using

a strained Hamiltonian as a perturbative term. A band edge model of m-Si is obtained, including dependence of CB/VB edge levels, indirect bandgap, and CB/VB splitting energy on  $x$ , which can supply valuable references for device design.

### 2 Deformation potentials

The effect of strain on the electronic system of a semiconductor may be modeled using the deformation potential theory. Strain is incorporated into the band-structure as a perturbed term in the calculation. The Hamiltonian of this perturbation,  $H_\epsilon$ , has matrix elements of the form<sup>[4]</sup>:

$$H_{\epsilon;ij} = \sum_{\alpha,\beta=1}^3 D_{ij}^{\alpha\beta} \epsilon_{\alpha\beta} \quad (1)$$

where  $\epsilon_{\alpha\beta}$  is the element of the strain tensor and  $D_{ij}^{\alpha\beta}$  is the deformation potential. The strain tensor for the (101) substrate can be obtained by the following formulae<sup>[5]</sup>.

$$\epsilon_{\square} = (a_{\text{Si}_{1-x}\text{Ge}_x} - a_{\text{Si}}) / a_{\text{Si}} \quad (2)$$

$$\epsilon_{xx} = \epsilon_{zz} = 1/2[1 - 1/\sigma^{(101)}] \epsilon_{\square}$$

$$\epsilon_{xy} = -1/2[1 + 1/\sigma^{(101)}] \epsilon_{\square} \quad (3)$$

$$\epsilon_{yz} = \epsilon_{zx} = 0$$

$$\epsilon_{yy} = \epsilon_{\square} \quad (4)$$

where the SiGe lattice constant  $a_{\text{Si}_{1-x}\text{Ge}_x}$  is obtained by linear interpolation.

First, the perturbed Hamiltonian of the  $\Delta$  conduction band (CB) is considered. Since the levels of CB are nondegenerate, the  $D^{\alpha\beta}$  are diagonal in  $(i, j)$

\* Project supported by the National Ministries and Commissions of China (Nos. 51308040203, 9140A08060407DZ0103)

<sup>†</sup> Corresponding author. Email: wmsjhsong@tom.com

Received 14 March 2008, revised manuscript received 5 May 2008

and may be treated as individual deformation potential constants. The  $\Delta$  CB minima are characterized by constant energy surfaces, which are ellipsoids of revolution whose major axes lie along their respective  $\langle 100 \rangle$  axes. Accounting for the three distinct  $\Delta$  levels, symmetry under rotation about  $[100]$ ,  $[010]$ , and  $[001]$  shows that respective  $H_\epsilon$  can be determined by the following equations:

$$H_{\epsilon, \langle 100 \rangle} = D^{xx} \epsilon_{xx} + D^{yy} (\epsilon_{yy} + \epsilon_{zz}) \quad (5)$$

$$H_{\epsilon, \langle 010 \rangle} = D^{xx} \epsilon_{yy} + D^{yy} (\epsilon_{xx} + \epsilon_{zz}) \quad (6)$$

$$H_{\epsilon, \langle 001 \rangle} = D^{xx} \epsilon_{zz} + D^{yy} (\epsilon_{xx} + \epsilon_{yy}) \quad (7)$$

where

$$D^{xx} = \Xi_d^\Delta + \Xi_u^\Delta \quad (8)$$

$$D^{yy} = \Xi_d^\Delta$$

$$H' = \begin{bmatrix} l\epsilon_{xx} + m(\epsilon_{yy} + \epsilon_{zz}) & n\epsilon_{xy} & n\epsilon_{zx} \\ n\epsilon_{xy} & l\epsilon_{yy} + m(\epsilon_{xx} + \epsilon_{zz}) & n\epsilon_{yz} \\ n\epsilon_{zx} & n\epsilon_{yz} & l\epsilon_{zz} + m(\epsilon_{yy} + \epsilon_{xx}) \end{bmatrix} \quad (11)$$

The notation  $x, y, z$  refers to the basis functions with the corresponding rotational symmetry of the  $\Gamma_{25}'$  representation of the symmetry group of the top of the VB. The up and down arrows denote spin up and down, respectively.

In order to discuss the nature of the VB, it is convenient to transform the original basis of  $|i_\alpha\rangle$  to our familiar basis of  $|j, m_j\rangle$ , which will make the description of the VB eigenstates clearer. The transformation matrix is:

$$U = \begin{bmatrix} -\frac{1}{\sqrt{2}} & 0 & 0 & 0 & \frac{1}{\sqrt{6}} & \frac{1}{\sqrt{3}} \\ -\frac{i}{\sqrt{2}} & 0 & 0 & 0 & -\frac{i}{\sqrt{6}} & -\frac{i}{\sqrt{3}} \\ 0 & \frac{2}{\sqrt{6}} & -\frac{1}{\sqrt{3}} & 0 & 0 & 0 \\ 0 & -\frac{1}{\sqrt{6}} & -\frac{1}{\sqrt{3}} & -\frac{1}{\sqrt{2}} & 0 & 0 \\ 0 & -\frac{i}{\sqrt{6}} & -\frac{i}{\sqrt{3}} & \frac{i}{\sqrt{2}} & 0 & 0 \\ 0 & 0 & 0 & 0 & \frac{2}{\sqrt{6}} & -\frac{1}{\sqrt{3}} \end{bmatrix} \quad (12)$$

The strain Hamiltonian written in the  $JM_J$  representation can now be expressed as

$$H_{\epsilon, jm_j} = U^{-1} H_{\epsilon, i\alpha} U \quad (13)$$

Table 1 Values used in the calculation

Parameter	Symbol (unit)	Value Reference
Si lattice constant	$a_0$ (nm)	0.357 nm [7]
Ge lattice constant	$a_0$ (nm)	0.357 nm [7]
Poisson's ratio	$\sigma^{(101)}$	1.959 [8]
Deformation potential	$\Xi_d^\Delta$ (eV)	1.75 [9]
Deformation potential	$\Xi_u^\Delta$ (eV)	9.16 [9]
Deformation potential	$l$	-0.15 [10]
Deformation potential	$m$	6.84 [10]
Deformation potential	$n$	-5.89 [10]

For m-Si, substituting Eq. (3) into Eqs. (5) ~ (8), we get,

$$H_{\epsilon, \langle 100 \rangle} = H_{\epsilon, \langle 001 \rangle} = \Xi_d^\Delta (\epsilon_{xx} + \epsilon_{yy} + \epsilon_{zz}) + \Xi_u^\Delta \epsilon_{xx} \quad (9)$$

$$H_{\epsilon, \langle 010 \rangle} = \Xi_d^\Delta (\epsilon_{xx} + \epsilon_{yy} + \epsilon_{zz}) + \Xi_u^\Delta \epsilon_{yy}$$

The valence band (VB) deformation potential theory proves to be qualitatively different than that of the CB due to the three-fold degeneracy of the  $\Gamma_{25}'$  representation for each spin orientation. Analogous to the  $k \cdot p$  Hamiltonian matrix of the top of the VB, the strained Hamiltonian in  $i\alpha$  representation ( $i = x, y, z, \alpha = \uparrow, \downarrow$ ) [6] is:

$$H_{\epsilon, i\alpha} = \begin{bmatrix} H' & 0_{3 \times 3} \\ 0_{3 \times 3} & H' \end{bmatrix} \begin{matrix} \uparrow \\ \downarrow \end{matrix} \quad (10)$$

### 3 Results and discussion

As mentioned above, the strain-induced energy shift ( $\delta E$ ) in CB may be determined by Eq. (9). The CB edge level in m-Si can be obtained by

$$E_C = E_c^0 + \delta E \quad (14)$$

where the value of  $E_c^0$ , i.e., the CB edge of unstrained Si, is 1.119 eV. The dependence of the CB edge on the Ge fraction ( $x$ ) is shown in Fig. 1. The CB edge is characterized by the same four valleys splitting from the  $[010]$ ,  $[0\bar{1}0]$  valleys, or  $[001]$ ,  $[00\bar{1}]$ ,  $[100]$ ,  $[\bar{1}00]$  valleys, which are shifted upward in energy. The dependence of CB splitting energy between  $\Delta_2$  and  $\Delta_4$  valleys on  $x$  is plotted in Fig. 2. The results above can be interpreted from the force diagram of the six  $\Delta$  valleys, as shown in Fig. 3. The growth on a substrate of the orientation (101) considered in this work produces a monoclinic distortion and splits the six  $\Delta$  valleys.

The effect of spin-orbit coupling ( $H_{so}$ ) and the effects of strain ( $H_{\epsilon, |j, m_j\rangle}$ ) are added to the zero point

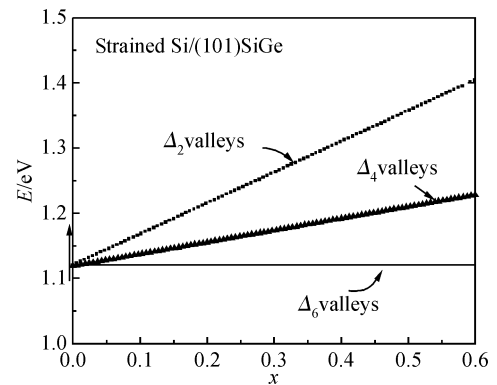


Fig. 1 CB edge versus Ge fraction ( $x$ ) in m-Si

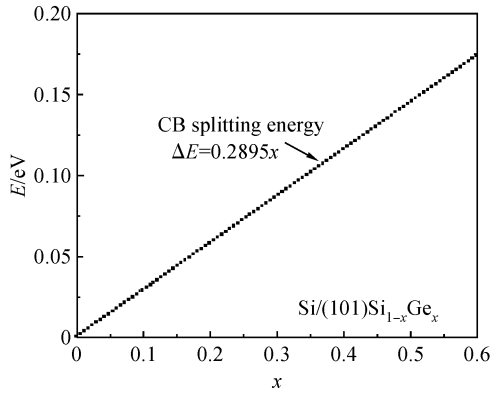


Fig. 2 CB splitting energy versus Ge fraction ( $x$ ) in m-Si

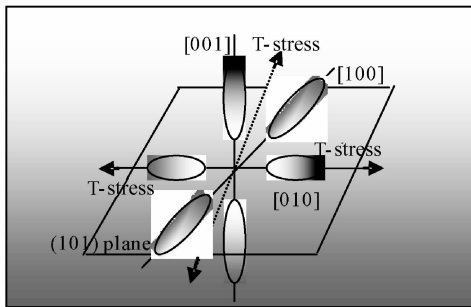


Fig. 3 Schematic equi-energy surfaces of the six split valleys in the first CB in m-Si

to get the position of VB near the center of the Brillouin zone:

$$E_v^i = E_v^0 + \langle J, m_j | H_{so} + H_{\epsilon, j m_j} | J, m_j \rangle \quad (15)$$

where the value of  $E_v^0$ , i. e., the VB edge of unstrained Si is zero. In the  $JM_J$  representation,  $H_{so}$  has the form:

$$H_{so} = \begin{bmatrix} \Delta/3 & 0 & 0 & 0 & 0 & 0 \\ 0 & \Delta/3 & 0 & 0 & 0 & 0 \\ 0 & 0 & -2\Delta/3 & 0 & 0 & 0 \\ 0 & 0 & 0 & \Delta/3 & 0 & 0 \\ 0 & 0 & 0 & 0 & \Delta/3 & 0 \\ 0 & 0 & 0 & 0 & 0 & -2\Delta/3 \end{bmatrix} \quad (16)$$

The calculated results have been plotted in Fig. 4. The

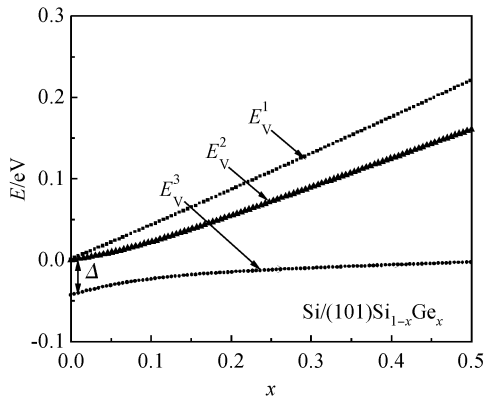


Fig. 4 VB edge versus Ge fraction ( $x$ ) in m-Si where  $\Delta$  is the splitting energy and its value is 0.044eV

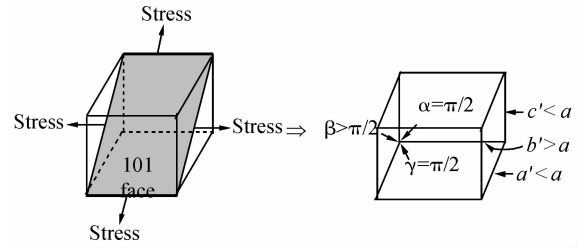


Fig. 5 Schematic cell structure of strained Si on (101)Si<sub>1-x</sub>Ge<sub>x</sub> where  $a', b', c', \alpha, \beta, \gamma$  are the lattice constants under strain

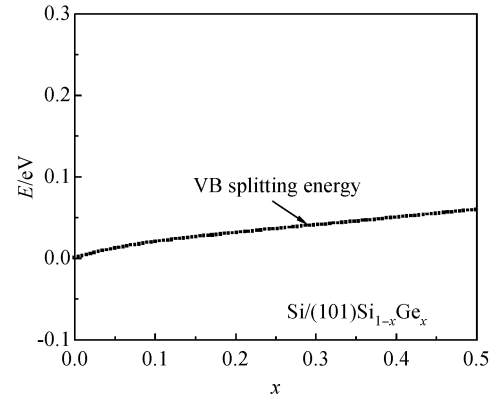


Fig. 6 VB splitting energy versus Ge fraction ( $x$ ) in m-Si

splitting of the first and second VB occurs and all VB edges move up in electron energy as the Ge fraction ( $x$ ) increases. This is attributed to the following fact: Under the biaxial tensile stress imposed by the (101) substrate, a form transformation of the Si epitaxial layer from cubic to monoclinic occurs (seen in Fig. 5), which causes lower symmetry, and hence lifts the VB edge degeneracy.

In view of the applications and the efficient design of devices, the VB splitting energy between the top and second bands at  $k = 0$  and the indirect bandgap are plotted as a function of  $x$ . The result is shown in Fig. 6 and Fig. 7.

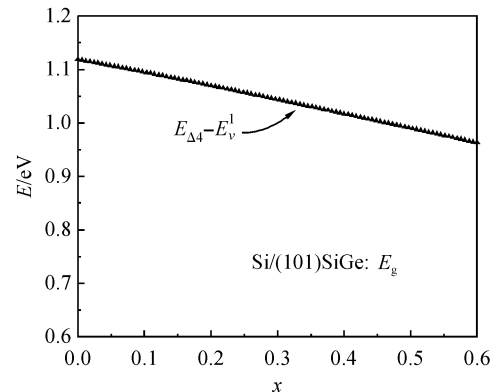


Fig. 7 Indirect bandgap versus Ge fraction ( $x$ ) in m-Si

## 4 Conclusion

We have systematically investigated the band edge levels in (101)-biaxial strained Si on relaxed  $\text{Si}_{1-x}\text{Ge}_x$  alloy, or monoclinic Si (m-Si), using the  $k \cdot p$  perturbation method coupled with deformation potential theory. The main results of this paper can be deduced from Figs. 1~7. Noticeably, both the bottom CB and the top VB edge levels move up in electron energy as the Ge fraction ( $x$ ) increases. In addition, the dependence of the CB edge splitting energy between  $\Delta_2$  and  $\Delta_4$  valleys, the VB edge splitting energy between the top and second bands at  $k = 0$ , and the indirect bandgap on  $x$  were plotted. The decrease in the indirect bandgap and the increase in the CB/VB edge splitting energy as  $x$  increased were found.

## References

[1] Hu Huiyong, Zhang Heming, Jia Xinzhang, et al. Study on Si-SiGe

three-dimension CMOS integrant circuits. Chinese Journal of Semiconductors, 2007, 28(5):36

- [2] Watling J R, Yang L, Borici M, et al. The impact of interface roughness scattering and degeneracy in relaxed and strained Si n-channel MOSFETs. Solid-State Electron, 2004, 48:1337
- [3] Chattopadhyay S, Driscoll L D, Kwa K S K, et al. Strained Si MOSFETs on relaxed SiGe platforms: performance and challenges. Solid-State Electron, 2004, 48:1407
- [4] Bir G L, Pikus G E. Symmetry and strain induced effects in semiconductors. New York: John Wiley & Sons, 1974
- [5] Smirnov S, Kosina H. Monte Carlo modeling of the electron mobility in strained  $\text{Si}_{1-x}\text{Ge}_x$  layers on arbitrarily oriented  $\text{Si}_{1-y}\text{Ge}_y$  substrates. Solid-State Electron, 2004, 48:1325
- [6] Manku T, Nathan A. Energy-band structure for strained p-type  $\text{Si}_{1-x}\text{Ge}_x$ . Appl Phys, 1991, 43(15):12634
- [7] Levinshtein M E, Rumyantsev S L, Shur M S. Properties of advanced semiconductor materials. New York: John Wiley & Sons, 2001
- [8] Fischetti M V, Laux S E. Band structure, deformation potential and carrier mobility in strained Si, Ge and SiGe alloy. Appl Phys, 1996, 80(4):2234
- [9] Kasper E. Properties of strained and relaxed silicon germanium. Beijing: National Defense Industry Press, 2002
- [10] Hinckley J M. The effect of strain in pseudomorphic p- $\text{Si}_{1-x}\text{Ge}_x$ . Michigan: The University of Michigan, 1990

## (101)面生长双轴应变 Si 带边模型\*

宋建军<sup>†</sup> 张鹤鸣 戴显英 胡辉勇 宣荣喜

(西安电子科技大学微电子学院, 宽禁带半导体材料与器件教育部重点实验室, 西安 710071)

**摘要:** 采用结合形变势理论的  $k \cdot p$  微扰法建立了(101)面弛豫  $\text{Si}_{1-x}\text{Ge}_x$  衬底上生长的双轴应变 Si 的带边模型. 结果表明: [001], [00 $\bar{1}$ ], [100]及[ $\bar{1}$ 00]方向能谷构成了该应变 Si 的导带带边, 其能量值随 Ge 组分的增加而增加; 导带劈裂能与 Ge 组分成正比例线性关系; 价带三个带边能级都随 Ge 组分的增加而增加, 而且 Ge 组分越高价带带边劈裂能值越大; 禁带宽度随着 Ge 组分的增加而变小. 该模型可获得量化的数据, 为器件研究设计提供有价值的参考.

**关键词:** 应变 Si; 带边;  $k \cdot p$  法

**PACC:** 7360F; 7125C; 7115M

**中图分类号:** O471.5      **文献标识码:** A      **文章编号:** 0253-4177(2008)09-1670-04

\* 国家部委资助项目(批准号: 51308040203, 9140A08060407DZ0103)

<sup>†</sup> 通信作者. Email: wmsong@tom.com

2008-03-14 收到, 2008-05-05 定稿